Dielectric losses measured in a sodium aluminosilicate glass by using electrical insulating barriers and non-isothermal experimental conditions

F. Henn [a],[*], G. Garcia-Belmonte [b], J. Bisquert [b], S. Devautour-Vinot [a], J.C. Giuntini [a]

[a] Institut Charles Gerhardt, UMR-CNRS 5253, Université Montpellier 2, Place E. Bataillon, 34095 Montpellier cedex 5, France
[b] Departament de Física, Universitat Jaume I, 12071 Castelló, Spain

ARTICLE INFO

ABSTRACT

Ac conductivity and dielectric losses are measured on a sodium aluminosilicate glass using various experimental conditions. Data obtained using metallic contacts and insulating barriers are compared. The influences of the thermal environment, i.e. iso versus non-isothermal, and of the application of a constant dc electric field, i.e. BIAS, are also investigated. It is thus shown that the use of non-isothermal conditions and insulating barriers is a convenient tool for extracting and hence for analyzing the bulk intrinsic polarization response of the sample. The analysis of this response with a simple model based on distribution of energy barriers gives some insights into the glass structure which turns out to be rather homogeneous.

© 2008 Elsevier B.V. All rights reserved.

1. Introduction

Solid ionic conductors have been extensively studied in the last decades due to their ability to conduct electrical current caused by ionic motion. This phenomenon is dominant in solid state electrolytes for rechargeable batteries or fuel cells, sensors, ion exchange membranes, etc. and hence is crucial for numerous practical applications [1,2]. Meanwhile, the understanding of ion motion in solids and more particularly in glasses is still under debate and, so far, no universal model exists to account for the broad diversity [3–6] in experimental behavior. Further investigations focussed on the fundamental aspects of ionic conductivity in solids are therefore needed.

The atomic structure of the ionic glassy conductors is formed by a relatively rigid charged matrix on the one hand and ions of opposite charge occupying potential minima on the other hand. The ions are able to diffuse through the matrix by means of thermally activated hops between different potential minima. Depending on the time scale at which the ionic current density is measured, one may observe either (i) long-range redistribution of ions that gives rise to ion diffusion or dc conductivity or (ii) local ionic rearrangements causing dipolar reorientation and thus resulting in the intrinsic bulk polarization. In most cases, it is experimentally observed that the so-called Barton–Nakajima–Namikawa (BNN) proportionality [7,8]:

$$\sigma_{dc} = p\varepsilon_0\Delta\varepsilon\omega_c, \tag{1}$$

relates excess polarization (or dielectric strength) $\Delta\varepsilon$ and dc conductivity σ_{dc}. In Eq. (1), p is a proportionality parameter of the order of 1, and ω_c the frequency characterizing the threshold between local polarization to non local dc conductivity contributions. Eq. (1) would suggest that dc conduction and excess of polarization share the same physical origin, i.e. redistribution of ion position. Although both long and short range ionic redistribution rely on the same microscopic ion hopping process, the former is more likely to be a cooperative phenomenon related to strongly coupled hops while the latter one can be assumed as resulting from a superimposition of individual or localized, i.e. limited in a finite volume [9], independent ionic hops taking place throughout the glassy network. In this sense, analysis of the intrinsic bulk polarization in ionic conductors is expected to provide information about the localized ion hopping mechanism and hence about the microscopic glass structure [9,10].

In this paper, we aim at providing new experimental insights in the intrinsic polarization behavior of ionically conducting glasses by investigating the dielectric losses measured under non-isother-

mal conditions in the case of a test case sodium aluminosilicate glass 'sandwiched' between electrical insulating barriers. The studied glass is Na_2O–$0.4Al_2O_3$–$2.2SiO_2$ and the electrical barriers are thin films, i.e. 10 μm, of PolyTetraFluoroEthylene (PTFE also known as Teflon).

The structure of the paper is the following. In Section 2, we briefly recall the main features of the dielectric response of ionic glasses on the one hand, and on the other hand, the reasons that led us to use insulating barriers and non-isothermal conditions for studying the intrinsic bulk polarization of the sample. In Section 3, we report and discuss the experimental data thus obtained. A comparison between dielectric losses measured using isothermal and non-isothermal conditions is given as well as a detailed analysis of the data obtained when the sample is submitted to different experimental conditions: heating versus cooling ramp and BIAS versus no BIAS. Data analysis and discussion are given, before conclusion, in Section 4.

2. General features of dielectric losses (or ac conductivity) in ionic glasses and proposal for using insulating barriers and non-isothermal conditions

The intrinsic disordered environment of charge carriers, i.e. ions, in glasses is believed to give rise to distributed hopping mechanisms such as the usually observed frequency-dependent conductivity $\sigma'_{pol}(\omega)$ which obeys an approximate power-law of the type [11–14]:

$$\sigma'_{pol}(\omega) \propto \omega^s, \tag{2}$$

where the exponent s is usually comprised between 0.5 and 1. It must be emphasized at that point that the parameter s is not strictly constant but a increasing function of frequency at a given fixed temperature.

So, in common to many other disordered materials, the high frequency domain of the ac conductivity spectrum $\sigma'_{ac}(\omega)$ of ionic oxide glasses is found to follow Eq. (2) while at low frequencies it exhibits the frequency independent behavior (Fig. 1(a)) related to dc conductivity σ_{dc}. The transition from σ_{dc} to $\sigma'(\omega)$ is marked by the characteristic frequency ω_c (Fig. 1(a)). For frequencies $\omega \ll \omega_c$, conduction appears to be homogeneous at all spatial scales as expected for ordinary (Fickean) diffusion, while for $\omega \gg \omega_c$ the ions move following a sub-diffusive regime [15,16], featured by the exponent s (Eq. (2)), which can be related to the bulk intrinsic polarization. If one assumes $\sigma'_{pol}(\omega)$ arises from the superposition of localized thermally activated ionic hops characterized by a relaxation time τ_{pol} and hence by the associated energy barrier ΔE_{pol}:

$$\tau_{pol} = \tau_0 \cdot \exp\left(\frac{\Delta E_{pol}}{kT}\right), \tag{3}$$

then the power-law parameter s can be seen as resulting from the shape of the distribution function of relaxation times. Moreover, if s is a decreasing function of temperature then it can be assumed that the distribution function of relaxation time results from a distribution of energy barriers ΔE_{pol}. In Eq. (3), the pre-exponential term τ_0 is a constant related to the ion hopping attempt frequency $\omega_0 (\omega_0 = \tau_0^{-1})$ which is in the order of 10^{13} s^{-1}, k the Boltzman constant and T the temperature.

When investigating polarization, it can be more convenient to plot the experimental data using the complex permittivity representation providing that dielectric losses $\varepsilon''_{ac}(\omega)$ are related to $\sigma'_{ac}(\omega)$ via:

$$\varepsilon''_{ac}(\omega) = \frac{\sigma'_{ac}(\omega)}{\varepsilon_0} \cdot \omega^{-1}. \tag{4}$$
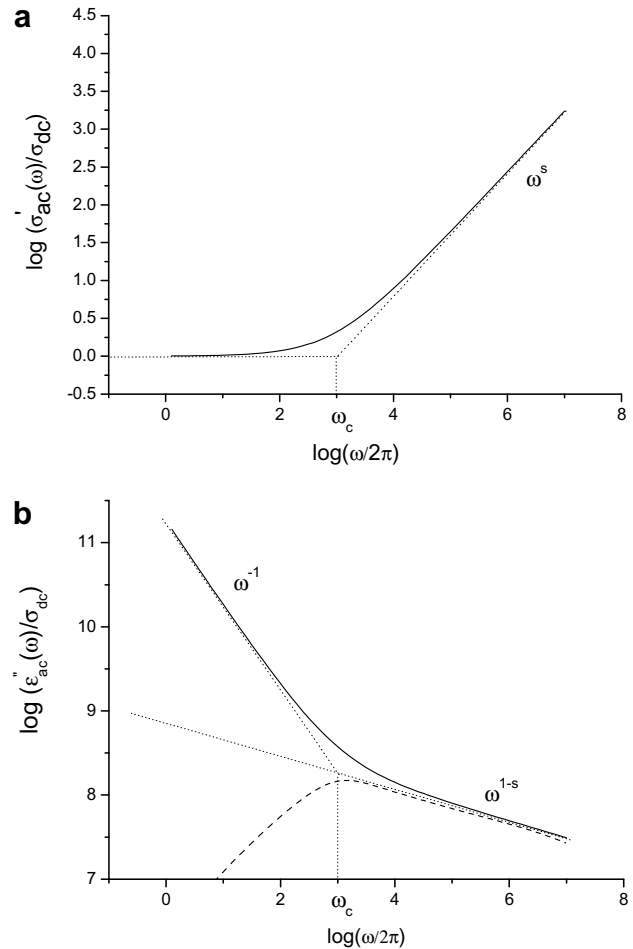
Fig. 1. Schematic log–log representation (normalized to dc conductivity σ_{dc}) of the ac conductivity $\sigma'_{ac}(\omega)$ (a) and the corresponding dielectric losses $\varepsilon''_{ac}(\omega)$ (see Eq. (2)) (b) spectra as a function of frequency, $f = \omega/2\pi$, in ionically conducting glasses. Dash line would represent the signal if no dc contribution occured.

Then, it follows from Eqs. (2) and (4) that $\varepsilon''_{ac}(\omega)$ obeys, at high frequency, a power-law of the type $\varepsilon''_{pol}(\omega) \propto \omega^{s-1}$ whereas, at low frequency, σ_{dc} dominates and $\varepsilon''_{ac}(\omega)$ follows ω^{-1} (Fig. 1(b)). If ionic glasses behaved as pure dielectric materials, i.e. with no dc conductivity σ_{dc}, $\varepsilon''_{ac}(\omega)$ would exhibit a peak where the maximum would correspond to the resonant frequency of the dipolar relaxation associated to the predominant ion hopping barrier (Fig. 1(b)). As far as we know, this behavior has never been observed. However, as schematized in Fig. 1b, it has been reported that the frequency of the $\varepsilon''_{ac}(\omega)$ peak that can be visualized from a Kramers–Kronig transformation of the real part $\varepsilon'_{ac}(\omega)$ [16], was strongly related to the characteristic frequency ω_c, i.e. to its activation energy ΔE_c.

Nevertheless, it must be emphasized that the ω^{-1} contribution, i.e. σ_{dc}, governs the ac response over a large frequency domain so that the detailed investigation of the polarization contribution $\varepsilon''_{pol}(\omega)$ and hence the exact determination of ω_c can be tricky. Furthermore, the blocking of ions at the surface of metallic electrode creates an interfacial polarization which also strongly modifies the shape of the ac conductivity (or permittivity) spectrum thus making the extraction of the $\varepsilon''_{pol}(\omega)$ contribution even more problematic.

In order to discard this drawback and thus to make the investigation of $\varepsilon''_{pol}(\omega)$ more reliable some of us have proposed [17] to study the ac electrical response of ionically conducting

materials by placing the sample between two insulating barriers. By insulating barriers, we mean materials that can be considered as pure dielectrics, i.e. materials which the resistance is high enough to ensure that no polarization relaxation occurs in the investigated time (or frequency) domain. In the present study, the insulating barriers are made of thin (10 μm) PTFE films. The basic idea behind this proposal is that no direct current can thus flow through the sample and, hence, that interfacial polarization effects can be limited as much as possible. However, it results from the arrangement in series of the insulating barriers, i.e. capacitances, with the sample dc conductivity a dielectric losses peak which the single Debye, i.e. lorentzian, contribution partly overlaps to the sample dielectric response. It can thus be demonstrated from a RC circuit representation that depending on the sample resistance, i.e. its geometry, the intensity of the Debye-like relaxation induced by the set-up is such that the shape of the bulk intrinsic polarization response $\varepsilon''_{pol}(\omega)$ extracted from the measured $\varepsilon''_{ac}(\omega)$ spectrum can be significantly altered.

More recently, some of us suggested [18] to improve this method by using non-isothermal measurements. In this case, the dielectric response is measured upon varying temperature conditions, e.g. heating or cooling, while the measurement frequency is maintained constant. The spectrum thus obtained is noted $\varepsilon''_{\omega_a,\pm q}(T)$ where ω_a is the fixed frequency and q the linear heating (+) or cooling (−) rate. This proposal was merely inspired from the basic principle of Thermally Stimulated Current spectroscopy [19,20] which was proven to be successfully when applied to ionic conductors [21–24]. For instance, it was shown in the case of a zeolite that the space-charge polarization due to the blocking of ions at the insulator/sample interface could be clearly separated out as long as the experimental parameters ω_a and q were properly adjusted [18]. It was also emphasized that the shape of the measured $\varepsilon''_{\omega_a,\pm q}(T)$ spectrum did not depend on the sample geometry in contrast to the isothermal $\varepsilon''_{ac}(\omega)$ spectrum.

In this work, we apply this method to a test case ionic glass, i.e $Na_2O–0.4Al_2O_3–2.2SiO_2$, in order to check whether the sample intrinsic dielectric signal $\varepsilon''^{(bulk)}_{\omega_a,\pm q}(T)$ can be appropriately extracted from the set-up experimental response and then, to see whether it corresponds to a standard polarization behavior which can be associated to the superposition of single localized ion hopping motions.

3. Experiments

3.1. Sample and dielectric measurement

The sample used in this work is an aluminosilicate ionic glass of chemical formula $Na_2O–0.4Al_2O_3–2.2SiO_2$ obtained by melting mixtures of $Na_2CO_3–10H_2O$, SiO_2 and Al_2O_3 in platinum crucibles in air at 1500 °C for 1 h and casting into ingots. Samples were annealed at 500 °C during 1 h, and then cooled to room temperature in order to remove internal mechanical stress due to quenching. The so-prepared piece of glass was shaped as a cylinder which diameter is 30 mm and thickness 2.1 mm. Its parallel faces were optically polished with diamond paste. Ac conductivity (or dielectric losses (Eq. (2))) measurements were performed, both under isothermal and non-isothermal conditions, using a Novocontrol Broad Band Dielectric Spectrometer.

When ac conductivity or dielectric losses were measured while the sample was not sandwiched between insulating barriers, the parallel faces of the sample were covered with a sputtered thin film of gold. When the sample was placed between insulating barriers, i.e. 10 μm thin films of PTFE, the sample faces were uncovered with gold electrodes.

Under isothermal condition, the spectra were recorded between 0.1 Hz and 2 MHz every 20 K from 273 K to 473 K. Under non-isothermal condition, the explored temperature domain was 173–473 K. The sample temperature was first stabilized for 15 min at the starting temperature, i.e. 173 K or 473 K, and then heated or cooled at a given constant ramping rate q down or up to the ending temperature, i.e. 173 K or 473 K. Three fixed frequencies (ω_a = 1 Hz, 10 Hz, 10 kHz) and three ramping rates (q = 2, 5, 10 K min^{-1}) were tested. It was checked by comparing data obtained upon cooling or heating after several temperature cycles with or without isothermal step, i.e. rest time at the extreme temperatures, that the thermal history had no influence on the measured $\varepsilon''^{(bulk)}_{\omega_a}(T)$ spectra. Noteworthy, this result is not surprising since the temperature domain explored here is well below the glass transition, i.e. >800 K [18], of the studied glass so that its chemical and physical features are not significantly altered.

3.2. Isothermal conductivity and dielectric spectra

The sample was first studied under isothermal conditions with and without insulating barriers. We report in Fig. 2, the ac conductivity and dielectric losses spectra obtained without (Fig. 2(a)) and with (Fig. 2(b)) insulating barriers. As expected (see Fig. 2(a)), the ac conductivity spectra (Fig. 2(a)) exhibit a low frequency 'pseudo-plateau' partly corresponding to σ_{dc} and a high frequency con-
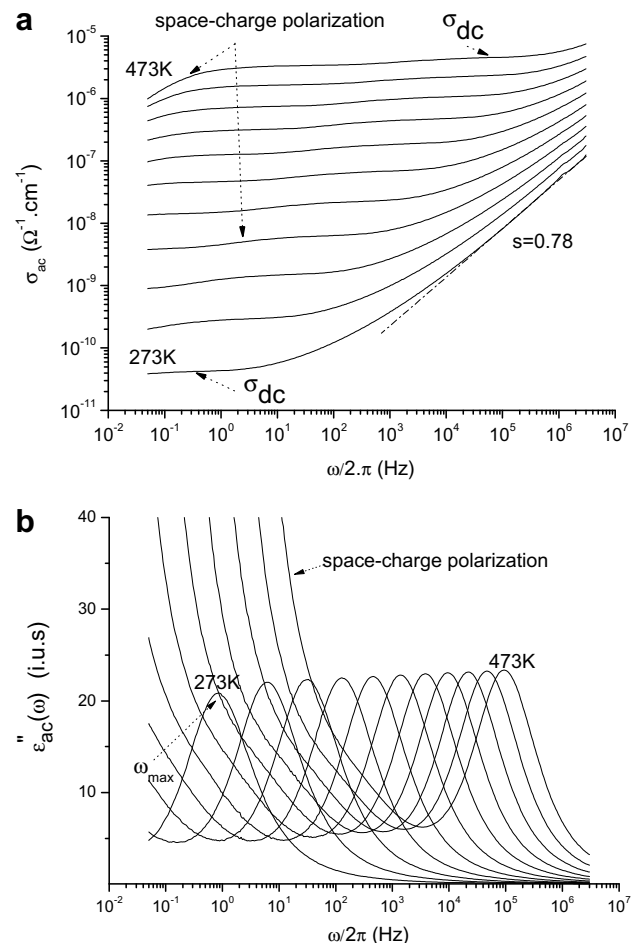

Fig. 2. Isothermal ac conductivity measured without insulating barriers (a) and dielectric losses obtained with insulating barrier (b) versus frequency. Spectra are recorded under isothermal condition every 20 K from 273 K to 473 K (full lines). The dash line in (a) features the high frequency ω^s contribution (Eq. (1)).

tribution $\sigma'_{pol}(\omega)$ obeying approximately Eq. (2) at low temperature. The low frequency behavior is called 'pseudo-plateau' since a more detailed analysis of the signal reveals a complex shape, i.e. not flat, which is commonly ascribed to electrode polarization due to ionic charge accumulation at the metallic contact/sample interface.

At high temperature, σ_{dc} becomes more and more predominant so that $\sigma'_{pol}(\omega)$ is not observable in the explored frequency range. Likewise, the unevenness of σ_{dc} appears more and more significant at low frequency. Nevertheless, an approximate determination of σ_{dc} is still possible by extracting the value of $\sigma'_{ac}(\omega)$ at the first inflection point as shown in Fig. 2(a). The parameter s, which can be determined at low temperature (Fig. 2(a)), appears to be equal to about 0.78 at 273 K. This value falls within the range of values usually reported in literature [3,14]. The temperature evolution of σ_{dc} follows an Arrhenius law (Fig. 2), i.e. $\sigma_{dc} = \sigma^0_{dc} \cdot \exp\left(\frac{-\Delta E_{dc}}{kT}\right)$, with $\sigma^0_{dc} = 310^3 \ \Omega^{-1} \ m^{-1}$ and $\Delta E_{dc} = 0.64$ eV. Again, these values are similar to those commonly reported for this type of ionic material [25].

The use of insulating barriers visibly suppresses the occurrence of the low frequency σ_{dc} contribution and hence, yields a dielectric loss peak with a maximum ω_{max} which increases with temperature (Fig. 2(b)). The increase of $\varepsilon''_{ac}(\omega)$ observed at low frequency can be ascribed, as for the unevenness of σ_{dc}, to interfacial space-charge polarization and thus emphasized that the use of thin insulating barriers does not totally prevent the accumulation of ionic charge at the metallic electrode/insulating barrier/ionic sample interface. Worth of noting, the use of thicker barriers that would reduce this undesirable electrode polarization would also significantly weaken the overall dielectric signal and thus would impede the measurement of the intrinsic bulk polarization contribution.

The temperature dependence of ω_{max} exhibits (Fig. 3), as for σ_{dc}, an Arrhenius behavior, i.e. $\omega_{max} = \omega^0_{max} \cdot \exp\left(\frac{-\Delta E_{\omega max}}{kT}\right)$, with $\Delta E_{\omega max} = 0.64$ eV and $\omega^0_{max} = 4.2 \times 10^{12} \ s^{-1}$. It is thus shown that $\Delta E_{\omega max} \cong \Delta E_{dc}$ and that ω^0_{max} is close to the expected value for ionic vibration.

The superposition of the spectra obtained at 273 K with and without insulating barrier is reported in Fig. 4(a). As an example, the low temperature spectra, i.e. 273 K, clearly show that the use of insulating barriers does not modify the high frequency domain where intrinsic polarization dominates. It can also be seen that ω_{max} does not equal ω_c when comparing the $\varepsilon''_{ac}(\omega)$ (Fig. 3) and $\sigma'_{ac}(\omega)$ (Fig. 1(a)) spectra obtained at 273 K. This absence of simple connection between ω_{max} and ω_c emphasizes that the determination of the later is not as simple as it might be expected from the drawing schematized in Fig. 1.
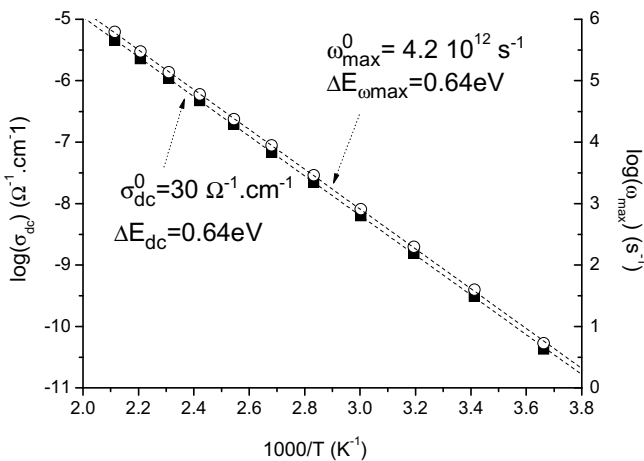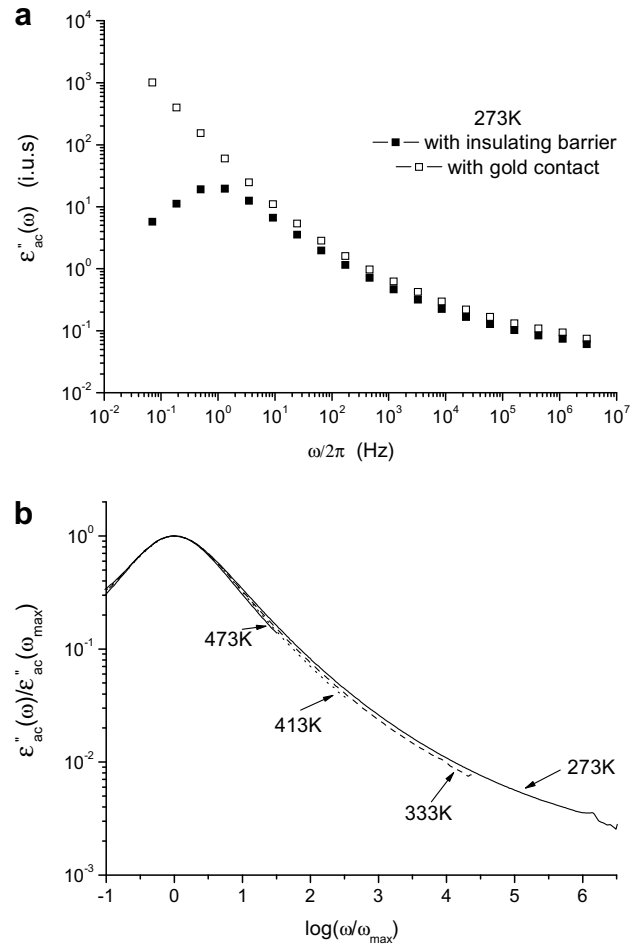

Fig. 4. Comparison of the dielectric losses spectra measured at 273 K with (full symbols) and without (open symbols) insulating barriers (a) and comparison of the dielectric losses spectra measured at different temperatures with insulating barriers and normalized to the coordinates of the signal peak (b).

On the other hand, it must also be emphasized that the various isothermal $\varepsilon''_{ac}(\omega)$ spectra (Fig. 2(b)) normalized to the peak coordinates cannot be rigorously superimposed (Fig. 4(b)) or, in other terms, that there is no master curve. The deviation which becomes more pronounced with the increasing frequency, i.e. the lower the

Fig. 3. Arrhenius plot of the dc conductivity (full square) and of the frequency of the dielectric peak (open circle). Dash lines represent the Arrhenius fits which yield the values of σ^0_{dc}, ΔE_{dc}, ω^0_{max} and $\Delta E_{\omega max}$.
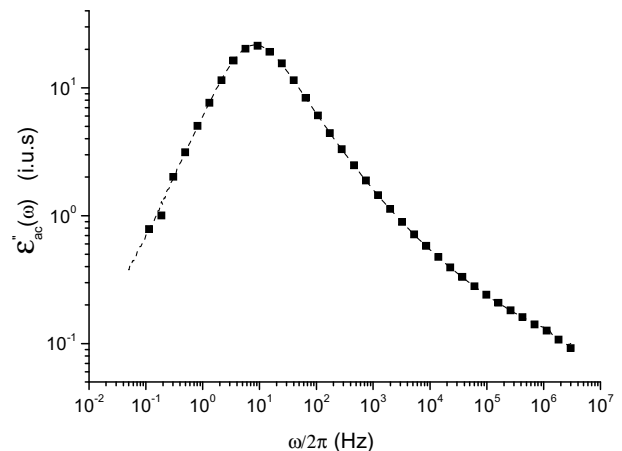

Fig. 5. Dielectric losses versus frequency spectra measured at 293 K using insulating barriers with (full square) or without (dash line) a BIAS (40 V).

temperature the larger the $\varepsilon''_{ac}(\omega)$ spectrum, indicates that the Time Temperature Superposition principle is not obeyed as one can expect from a system characterized by a distribution of energy barrier.

Finally, Fig. 5 shows that the application of a BIAS, i.e. 40 V, corresponding to a constant electric field of about 19 kV m^{-1} in the case studied here, does not influence at all the shape of the dielectric losses spectrum measured using insulating barrier. It can thus be assumed that the polarization phenomenon measured here is not influenced by any space-charge polarization effects which are known to be non-linear even for weak applied dc electric field.

3.3. Non-isothermal dielectric spectra

In the following, dielectric losses spectra were always measured using the sample/insulating barrier set-up.

3.3.1. Influence of the fixed frequency

First, we report the influence of the fixed frequency ω_a on the $\varepsilon''_{\omega_a,\pm q}(T)$ signal measured upon a linear heating ramp of 5 K min^{-1} (Fig. 6) when no BIAS is applied.

The non-isothermal dielectric response appears to be constituted of two distinct domains: a clearly defined peak at low temperature followed by a signal increase at high temperature. It is observed that in the explored temperature domain, i.e. 173–473 K, the $\varepsilon''_{\omega_a,\pm q}(T)$ peak is shifted toward lower temperature and becomes narrower when ω_a decreases as expected from a system characterized by a distribution of energy barrier (see Fig. 4(b)). This result is further confirmed by comparing (Fig. 6) data obtained from non-isothermal measurements to the corresponding isochronal points that can extracted from the isotherms reported in Fig. 2(b). The second observation that can be drawn from this comparison is that this accordance is only valid for the low temperature peak and not for the higher temperature domain in which the signal increases. Finally, a small but broad hump is sometime observed between the main peak at low temperature and the signal increase at high temperature. Noteworthy this hump is not always observed (see Figs. 6–8) and consequently cannot be considered as reproducible in position and intensity. We do not have detailed explanation for this phenomenon. The only assump-
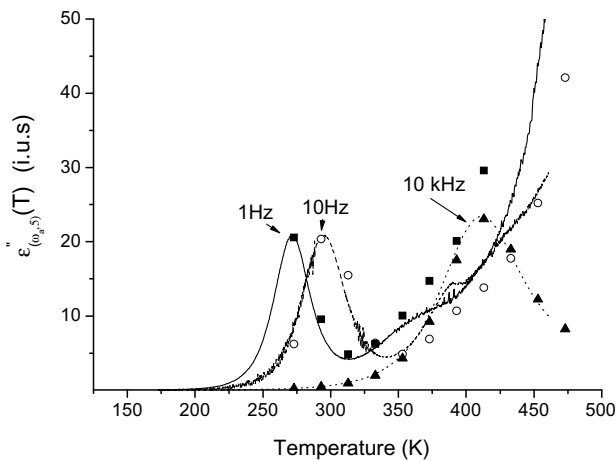
Fig. 7. Non-isothermal dielectric losses measured using insulating barriers and no BIAS for two fixed frequencies, i.e. 1 Hz (thin lines) and 10 Hz (thick lines), upon heating (full lines) and cooling (dash lines). Raw (a) and normalized to the peak coordinate (b) spectra.

Fig. 6. Non-isothermal dielectric losses measured using insulating barriers (and no BIAS) for three fixed frequencies 1 Hz (full line), 10 Hz (dash line) and 10 kHz (dot line) in the 173–473 K temperature domain upon a linear heating ramp of 5 K min^{-1}. The symbols correspond to the values of the dielectric losses obtained for a given frequency 1 Hz (full square), 10 Hz (open circle) and 10 kHz (full triangle) on various isotherms (Fig. 1(b)).
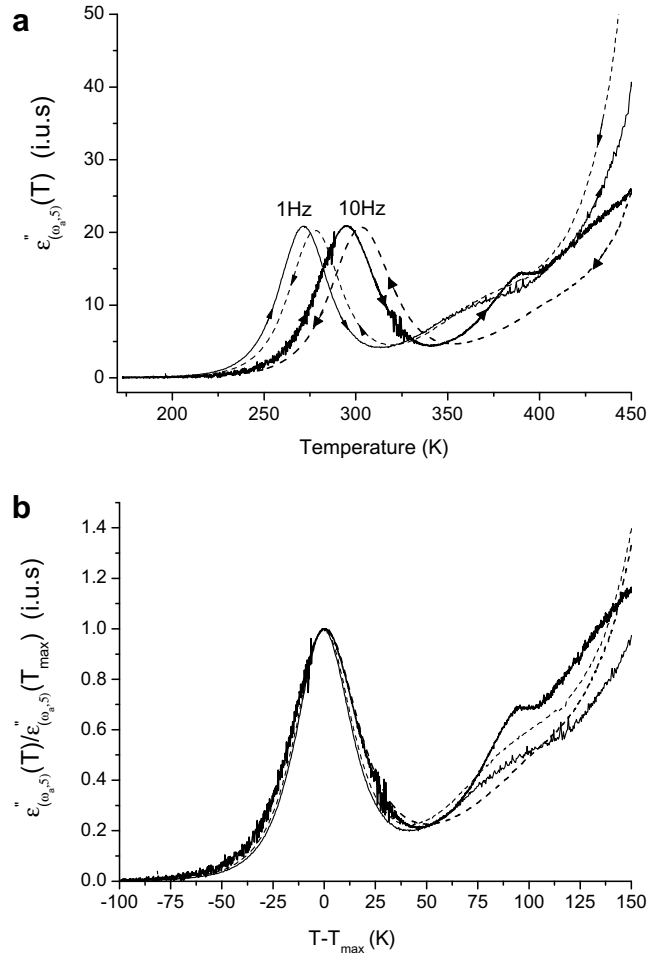

Fig. 8. Non-isothermal dielectric losses measured with insulating barriers with (dash line) and without (full line) application of a BIAS of 40 V. The fixed frequency is 1 Hz and the heating rate 5 K min^{-1}.

tion that could be proposed is that it is likely due to some polarization relaxation related to space-charge effect at the Teflon/ sample or metallic electrode/Teflon interface. A systematic study searching for the influence of the sample, metallic electrode and

PTFE surface state and of the pressure applied on the set-up by the metallic electrodes should provide insights in this experimental observation.

3.3.2. Effect of the ramping rate

Spectra recorded upon heating and cooling are compared for a given rate, i.e. $q = 5$ K min^{-1}, and for two values of ω_a in Figs. 7. It can then be seen that the peak maxima T_{max} occur systematically at higher temperature upon cooling than upon heating. This means that thermal ramping induces a gradient between the sample temperature T_{samp} and the temperature measured by the sensor T_{meas}. The temperature shift, noted $\Delta T_{max} = T_{max,cool} - T_{max,heat}$, is about 8 K for the two examples reported in Fig. 6(a). Providing that these maxima must correspond to the same relaxation time τ_{pol} imposed by the fixed frequency ω_a, i.e. $\tau_{pol} = \omega_a^{-1}$, Eq. (2) leads to $T_{samp} < T_{meas}$ upon cooling and oppositely to $T_{samp} > T_{meas}$ upon heating. It can thus be revealed from this observation that $T_{max,samp}$ corresponding to the sample intrinsic dielectric relaxation is comprised between the temperature maxima measured upon heating and cooling, so that the error on the determination of T_{samp} is at maximum equal to ΔT_{max}. In the case reported here as well as in the other experiments carried out in this work, ΔT_{max} never exceeds 10 K. We can therefore deduce from Eq. (2), i.e. $\Delta(\Delta E_{pol}) = k \cdot \ln\left(\frac{\omega_{max}^0}{\omega_a}\right) \cdot \Delta T_{max}$, that the maximum error which can be made on the value of the energy barrier ΔE_{pol} falls in the order of a few meV for the values of ω_a tested in this study. This error is therefore negligible in regards to the value of ΔE_{pol} which is in the order of 0.6 eV in the present case (Fig. 3).

However, it must be emphasized that the shape of the normalized $\varepsilon''_{\omega_a, \pm q}(T)$ peaks are, for a given value of ω_a, almost identical (Fig. 6(b)). This result emphasizes that the information contained in the $\varepsilon''_{\omega_a, \pm q}(T)$ peak is the same both upon heating and cooling. On the contrary, at high temperature the $\varepsilon''_{\omega_a, \pm q}(T)$ spectra cannot be superimposed (Fig. 7(b)), as expected for electrode polarization.

The influence of the heating rate, $q = 2, 5, 10$ K min^{-1}, for different values of ω_a, was then studied. The data (not reported here) yield exactly the same conclusion as those drawn from the experimental behavior reported in Figs. 6 and 7. The main outcome is again that the peaks of the normalized $\varepsilon''_{\omega_a, \pm q}(T)$ spectra can be superimposed whereas the high temperature part of the spectra cannot.

3.3.3. Effect of a BIAS

Finally, we studied the effect of a BIAS, i.e. 40 V, on the shape of the $\varepsilon''_{\omega_a, \pm q}(T)$ spectra. It can then be seen in Fig. 8 that the shape and the position of the peak are not altered whereas the application of a BIAS induces a significant raise of the signal at higher temperature. On the one hand, this outcome confirms that the high temperature part of the spectrum can be ascribed to space-charge polarization and on the other hand it shows that, at least in the case studied here, the use of a BIAS is not recommended since it significantly disturbs the high temperature part of the dielectric peak. Therefore, this result allows us to clearly isolate the part of dielectric spectra that must not be taken into account when analyzing the intrinsic polarization of the studied sample.

4. Discussion

The first and main important information which can be drawn from the data reported in Section 3 is that the use of insulating barriers and of non-isothermal condition for measuring dielectric losses allows us to clearly discriminate between a low temperature peak and a high temperature signal increase. The former exhibits the usual characteristics expected for a dielectric relaxation associated to a localized re-orientational mechanism: its shape does not

depend on the experimental conditions, i.e. heating versus cooling and ramping rate, and on the application of a constant dc electric field. On the contrary, the later is significantly altered by the experimental environments. It can therefore be concluded that it arises from complex polarization mechanism which corresponds to the building of capacitance due to the diffusion and thus of accumulation of ionic charges at the sample/insulating barriers. This phenomenon which implies long-range ionic diffusion is known to be very sensitive to the thermal history and to the application of an external constant electric field, i.e. BIAS. Noteworthy, such a space-charge polarization signal also occurs when no insulating barrier is used but, in that case, it is even more pronounced and less easily separated out from the intrinsic dipolar response.

It is also pointed out that the temperature shift resulting from the temperature gradient induced by non-isothermal condition yields a negligible error on the determination of ΔE_{pol}. Therefore, choosing appropriate ramping rate q and fixed frequency ω_a, the use of insulating barriers and non-isothermal conditions appears to be a convenient experimental tool to isolate the material dielectric response and consequently to analyze it with more confidence.

As an example, a more detailed analysis of the $\varepsilon''_{\omega_a, \pm q}(T)$ peak measured with $\omega_a = 1$ Hz and $q = 5$ K min^{-1} was carried out (Fig. 9). As already emphasized from the comparison of the various isothermal spectra, i.e. the absence of master curve (Fig. 4(b)), a simple model based of a distribution of energy barriers ΔE_{pol} was then assumed, so that the corresponding dielectric losses relaxa-
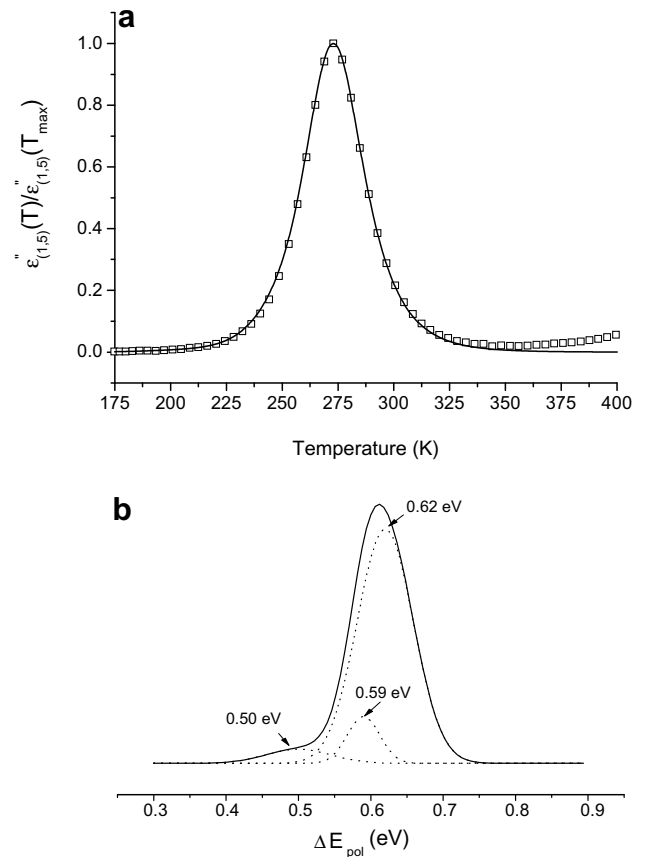
Fig. 9. Normalized non-isothermal dielectric losses measured using insulating barriers (open square) with $\omega_a = 1$ Hz and $q = 5$ K min^{-1} and fit (full line) using Eqs. (7) and (8) (see text) with $\tau_0 = 2.38 \times 10^{-13}$ s, $\Delta E^{\omega max} = 0.64$ eV and the distribution function plotted in (b) (a); distribution function of energy barriers, $g(\Delta E_{pol})$, which characterizes the material intrinsic dielectric response. $g(\Delta E_{pol})$ is decomposed in three Gaussian contributions (dot lines) (b).

tion function used for the fit of the experimental peak could be deduced from the following assumptions.

First, if the bulk response of the sample corresponds to that of an ensemble of independent ionic hops maintained at a constant temperature T, then dielectric losses relaxation function obeys:

$$\varepsilon''^{(\text{bulk})}_{\text{ac}}(\omega) = \int_0^\infty g(\ln \tau_{\text{pol}}, \Delta\varepsilon) \cdot \Delta\varepsilon \cdot \frac{\omega\tau_{\text{pol}}}{1 + \omega^2 \tau_{\text{pol}}^2} \, \mathrm{d}\tau_{\text{pol}}, \qquad (5)$$

where $g(\ln \tau_{\text{pol}}, \Delta\varepsilon)$ is the statistical weight of dipoles featured by the same relaxation time τ_{pol} and dielectric strength $\Delta\varepsilon$. Assuming, in first approximation, that all the dipoles have the same dielectric strength $\Delta\varepsilon$ and pre-exponential factor τ_0, Eq. (5) can be simplified so that using Eq. (2), the isothermal dielectric losses spectrum becomes:

$$\varepsilon''^{(\text{bulk})}_{\text{ac}}(\omega) = \Delta\varepsilon \cdot \int_0^\infty g(\Delta E_{\text{pol}}) \frac{\omega\tau_0 \exp\left(\frac{\Delta E_{\text{pol}}}{kT}\right)}{1 + \omega^2 \tau_0^2 \exp\left(\frac{2 \cdot \Delta E_{\text{pol}}}{kT}\right)} \, \mathrm{d}\Delta E_{\text{pol}}. \qquad (6)$$

Finally, $\Delta\varepsilon$ being weakly temperature dependent [9], the non-isothermal dielectric losses signal $\varepsilon''^{(\text{bulk})}_{\omega_a, \pm q}(T)$ due to the sample can be written as:

$$\varepsilon''^{(\text{bulk})}_{\omega_a, q}(T) = \Delta\varepsilon \cdot \int_0^\infty g(\Delta E_{\text{pol}}) \frac{\omega_a\tau_0 \exp\left(\frac{\Delta E_{\text{pol}}}{kT}\right)}{1 + \omega_a^2 \tau_0^2 \exp\left(\frac{2 \cdot \Delta E_{\text{pol}}}{kT}\right)} \, \mathrm{d}\Delta E_{\text{pol}}. \qquad (7)$$

The raw $\varepsilon''_{\omega_a, \pm q}(T)$ spectrum measured with the insulating barriers does not correspond to Eq. (7) since a Debye-like peak due to the set-up is added to the sample signal. It results that the raw spectrum follows:

$$\varepsilon''_{\omega_a, q}(T) = \varepsilon''^{(\text{bulk})}_{\omega_a, q}(T) + \Delta\varepsilon_{\text{barrier}} \cdot \frac{\omega_a\tau_0 \exp\left(\frac{\Delta E_{\omega\max}}{kT}\right)}{1 + \omega_a^2 \tau_0^2 \exp\left(\frac{2 \cdot \Delta E_{\omega\max}}{kT}\right)}, \qquad (8)$$

where $\Delta\varepsilon_{\text{barrier}}$ is the excess of polarization introduced by the insulating barrier.

The fit of the raw $\varepsilon''_{\omega_a, \pm q}(T)$ spectrum measured with ω_a = 1 Hz and q = 5 K min^{-1}, and normalized to 1 is plotted in Fig. 9. It is obtained by using Eqs. (7) and (8) with $\tau_0 = 2.38 \times 10^{-13}$ s (see text Section 3.2 and Fig. 2), $\Delta E_{\omega_{\max}} = 0.64$ eV and the distribution function reported in Fig. 9(b). The discrepancy observed at high temperature (Fig. 9(a)) can be assigned to the occurrence of space-charge polarization as revealed by data reported in Fig. 8.

A further analysis of the distribution function characterizing dielectric losses of the sodium aluminosilicate glass studied in this work shows that it can be decomposed in three Gaussians (Fig. 9(b)). According to our assumptions, i.e. the dielectric response corresponds to the superposition of individual dipolar reorientational motions, these contributions can be related to three different types of ionic hops. The weaker contribution is centered at 0.50 eV while the more important one is around 0.62 eV very close to the threshold value ΔE_c in connection with dc conductivity, i.e. 0.64 eV. Although the barriers are distributed, they do not differ very much from $\Delta E_{\sigma_{dc}}$, i.e. the distribution function is relatively narrow. This result is in full accordance with the fact that the superposition of the isothermal spectra (Fig. 4(b)) pointed out that their shape was slightly temperature dependent. The moderate spreading of the values of the energy barriers is not astonishing since one may expect from simple chemical considerations that the sodium cations are always engaged in Na$^+\cdots$O$^-$ bonds whose energies range in a limited energy domain accordingly to the solid framework chemical composition and topology. Meanwhile, the distribution obtained here is significant and clearly emphasizes that the sodium cation environment varies throughout the glassy structure. The lack of structural data for the glass studied here precludes a straightforward assignment for each Gaussian contribution. However, if we refer to similar investigations led on sodium crystalline aluminosilicates, i.e. zeolites [26], it can be supposed that these different types of cationic sites differ by the strength of the negative charge hold by the aluminosilicate framework and/or by the number of the oxygen atoms located in their surrounding. The oxygen atom negative charge is likely to increase with the number of aluminum atoms situated in the sodium site vicinity. Indeed, aluminum atoms being more electron donor than silicon ones, the oxygen atoms surrounding aluminum bear a stronger negative charge which induces more iononicity and consequently stronger sodium cation/glassy framework interaction. Furthermore, for a given number of aluminum atoms surrounding a given cationic site, one expect the shorter the Na$^+\cdots$O$^-$ bond the stronger the energy barrier for hopping.

Finally, it can be noticed (Fig. 9(b)) that the higher the energy barrier the larger the statistical weight. It means that the most probable cationic sites implicated in the sample intrinsic polarization resembles to those involved in dc conductivity. This result which is in accordance with the concepts of percolation and of energetic clusters [9] indicates that, in this glass, the cationic sites are rather well randomly distributed throughout the structure and hence that no preferred path with low energy barrier exits for dc conductivity. By considering the polarization model of energetic clustering, the energy distribution reported in Fig. 9(b) would entail that clusters are in fact small in size (containing a few sites for ion hopping). That is to say that such small-size clusters homogeneously occupy all the glass volume.

In order to verify this assumption, the cluster size L_c can be estimated from the energetic clustering model (see Eq. (12) in [9]):

$$L_c = \frac{e^2 x (1-x)}{3kT\varepsilon_0 \Delta\varepsilon}, \qquad (9)$$

where e is the cation elementary charge and x the molar alkali content, i.e. ~ 0.175 in the present case. The sample dielectric strength $\Delta\varepsilon$ is determined from the real part of permittivity $\varepsilon'_{\text{ac}}(\omega)$ spectrum measured under isothermal condition and with metallic contact to be equal to about 12 at 273 K (Fig. 10). Input in Eq. (8), it yields $L_c \approx 3$ nm. This result enforces our assumption that the polarizing domains are nanoscopic and hence, homogeneously distributed all over the glassy matrix.

Nevertheless these last derivations should be taken with caution because in the energy analysis conducted using Eqs. (7) and (8) two strong conditions have been imposed: similar dielectric
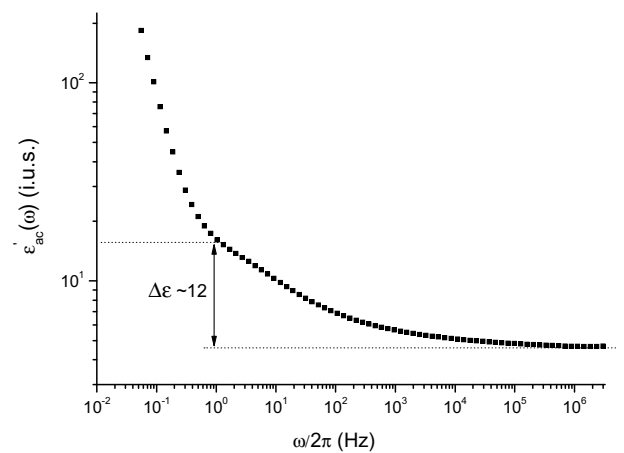

Fig. 10. Real part of permittivity versus frequency spectrum measured at 293 K using metallic contact. The dielectric strength $\Delta\varepsilon$ is the difference between the low and high frequency plateaus. The low frequency plateau corresponds to the sample dielectric constant. Being overlapped by the electrode polarization, the later can only be approximately determined by extrapolation at the point where the signal slope changes.

strength and non-correlated polarization (ensemble of independent ionic hops). These constraints are rather reasonable [27] when individual dipolar processes are regarded but seem not to be of straightforward application when the polarizing units, i.e. clusters, are bigger than elementary ion hopping between neighboring sites and when they are close to each others. Nevertheless, our experimental observations entails that cluster and elementary polarization share common trends, presumably because of the small cluster size as discussed above.

5. Conclusion

First of all, it is pointed out that from the proposed experimental methodology that is based on the combined use of insulating barriers and non-isothermal experimental conditions allows us to clearly separate the bulk intrinsic polarization relaxation from the extrinsic polarization induced by dc conductivity and the resulting blocking of cations at the sample/metallic electrodes interface. By choosing suitable experimental parameters: (i) heating or cooling rate, (ii) fixed measurement frequency and (iii) the application or not of a constant dc electric field (BIAS) superimposed to the ac field, it is thus possible to access and hence to analyze with more confidence, compared to the analysis of isothermal spectra, the bulk intrinsic polarization response of the studied sample. The combined use of insulating electrodes and of non-isothermal modus operandi thus provides experimental conditions of great interest for the investigation of bulk polarization in ionic materials.

In the case of the sodium aluminosilicate glass investigated here, the data obtained by using this methodology show that the intrinsic bulk response complies with a 'simple' linear dipolar behavior. This outcome supports the assumption that bulk polarization arises from the superimposition of local ionic re-arrangement via simple thermally activated hopping mechanism. Beyond the initial goal of this work, i.e. the development and refinement of a new methodology for measuring dielectric properties of ionically conducting solids, it is also shown that the determination of energy barriers involved in ion hopping mechanism can be used as a complementary mean for accessing information about the local framework structure where cations are embedded.

Although the signal analysis does not allow us a detailed examination of the glass structure, it shows that different types of cationic site, characterized by energy barriers ranging from 0.50 to 0.64 eV, exit in this glass. Noticeably, this result highlights the disorder character, which can be related to both chemical and topological aspects, around the sodium sites. Finally, it could be concluded from the fact that the activation energy for dc conductivity (0.64 eV) is very close to the most probable energy barrier that we can observe for the bulk polarization (0.62 eV) that no preferred, i.e. 'low barrier', long scale conduction path probably exists in this glass. This would mean that the structure of this glass is rather homogeneous or, in other terms, that the polarizing units larger than elementary ionic hops are small and homogeneously distributed throughout the sample. This conclusion is in full agreement with the size of the 'energetic' clusters, i.e. 3 nm, determined from the analysis of the dielectric strength measured on the same sample.

References

[1] P. Knauth, H. Tuller, J. Am. Ceram. Soc. 85 (2002) 1654.
[2] J.M. Tarascon, M. Armand, Nature 414 (2001) 359.
[3] J.R. Macdonald, M.M. Ahmad, J. Phys.: Condens. Matter 19 (2007) 46215.
[4] B. Roling, C. Martiny, Phys. Rev. Lett. 85 (2000) 1274.
[5] J.R. Dygas, Solid State Ionics 176 (2005) 2065.
[6] A.S. Nowick, W.-K. Lee, Solid State Ionics 38-30 (1988) 89.
[7] H. Namikawa, J. Non-Cryst. Solids 18 (1975) 173.
[8] D.L. Sidebottom, B. Roling, K. Funke, Phys. Rev. B 63 (2000) 024301.
[9] G. Garcia-Belmonte, F. Henn, J. Bisquert, Chem. Phys. 330 (2006) 13.
[10] S. Devautour, C.P. Varsamis, F. Henn, E.I. Kamitsos, J.C. Giuntini, J. Vanderschueren, J. Phys. Chem. B 105 (2001) 5657.
[11] A.K. Jonsher, Nature 267 (1977) 673.
[12] S.R. Elliott, F. Henn, J. Non-Cryst. Solids 116 (1990) 179.
[13] J.C. Dyre, T.B. Schroder, Rev. Mod. Phys. 72 (2000) 873.
[14] D.L. Sidebottom, Phys. Rev. Lett. 83 (1999) 983.
[15] B. Roling, C. Martiny, S. Brückner, Phys. Rev. B 63 (2001) art. 21420.
[16] B. Roling, C. Martiny, K. Funke, J. Non-Cryst. Solids 249 (1999) 201.
[17] F. Henn, J.C. Giuntini, J.V. Zanchetta, Phys. Rev. B 48 (1993) 573.
[18] S. Devautour, J.C. Giuntini, F. Henn, IEEE Trans. Dielect. Electric Insul. 11 (2004) 320.
[19] J. Vanderschueren, J. Gasiot, Thermally Stimulated Relaxation in Solids, Topics in Applied Physics, vol. 33, Springer, Berlin, 1979.
[20] J. Van Turnhout, J. Phys. D: Appl. Phys. 8 (1975) 268.
[21] S. Devautour, F. Henn, J.C. Giuntini, J.V. Zanchetta, J. Vanderschueren, J. Phys. D: Appl. Phys. 32 (1999) 147.
[22] S. Devautour, C.P. Varsamis, F. Henn, E.I. Kamitsos, J.C. Giuntini, J. Vanderschueren, J. Phys. Chem. B 105 (2001) 5657.
[23] H. Belarbi, A. Haouzi, J.C. Giuntini, J.M. Douillard, F. Henn, J. Colloid Interf. Sci. 308 (2007) 216.
[24] S. Devautour, J. Vanderschueren, J.C. Giuntini, F. Henn, J.V. Zanchetta, J. Appl. Phys. 82 (1997) 5057.
[25] J. Lee, T. Yano, S. Shibata, M. Yamane, J. Non-Cryst. Solids 246 (1999) 83.
[26] A. Nicolas, S. Devautour-Vinot, G. Maurin, J.C. Giuntini, F. Henn, Micropor. Mesopor. Mater. 109 (2008) 413.
[27] P. Jund, W. Kob, R. Jullien, Phys. Rev. B 64 (2001) 134303.